Nucleation and growth of droplets at a liquid-gas interface

A. A. Nepomnyashchy
Department of Mathematics and Minerva Center for Nonlinear Physics of Complex Systems, Technion- Israel Institute of Technology, Haifa 32000, Israel

A. A. Golovin, A. E. Tikhomirova, and V. A. Volpert
Department of Engineering Sciences and Applied Mathematics, Northwestern University, Evanston, Illinois 60208, USA
(Received 25 April 2006; revised manuscript received 20 June 2006; published 25 August 2006)

The nucleation of liquid droplets at a liquid-gas interface from a saturated vapor in the gas phase, as well as the droplet growth after the nucleation are studied. These two processes determine the formation of a regular hexagonal array of drops on the surface of an evaporating film of polymer solution that is used for the fabrication of polymer membranes with a regular microporous structure. The free-energy barrier for the nucleation of a droplet at a liquid-gas interface is found as a function of the droplet radius and the contact angles, and the critical nucleation radius is computed. It is shown that the heterogeneous nucleation is thermodynamically more preferable than the homogeneous one. The role of the line tension between the phases is also estimated. Further growth of a droplet nucleated at the liquid-gas interface is studied. Two growth mechanisms are considered: by the vapor diffusion flux from the gas phase and by the surface diffusion of the vapor molecules adsorbed at the liquid-gas interface outside the droplet. Two cases, corresponding to unsaturated and saturated condensation, are considered. The droplet growth is described by a free-boundary problem which is solved analytically and numerically. The droplet growth exponents at different stages of growth are found.

DOI: 10.1103/PhysRevE.74.021605 PACS number(s): 64.60.Qb, 68.43.Jk, 64.70.Fx

I. INTRODUCTION

Some time ago, an interesting process of self-assembly of highly regular microporous structures in polymer films was discovered [1–12]. In this process, a film of polymer solution with a volatile organic solvent is placed on a substrate and put in contact with a gas phase saturated with water vapor. Due to the solvent evaporation, the film surface is cooled which causes precipitation of microscopic water droplets at the gas-liquid interface. Unlike the usual "breath figures," the ensemble of the floating droplets remains monodisperse during their growth. Droplets do not coalesce but rather aggregate into "islands" that grow and finally form a densely packed "crystal" with a hexagonal lattice. After complete evaporation of the solvent, a solid polymer film with a regular microporous structure is formed. Such polymer films with highly regular microporous structure can be used as novel biointerfaces [13], photonic band gap devices [14,15], dichroic filters [16], picoliter beakers [11], and other interesting applications.

The key processes that determine the self-assembly of condensing water droplets at a liquid-gas interface are the nucleation of drops and their further growth. Droplet nucleation on a solid substrate (heterogeneous nucleation) and growth have been extensively studied [17–20]. It was shown that the radius of a single droplet at different growth stages increases with time according to a power law with different exponents that depend on the growth mechanism (diffusion or coalescence), the surface properties, geometry, etc. One of the growth mechanisms in heterogeneous nucleation is the diffusion flux from the vapor phase considered in detail in [19]. Another important droplet growth mechanism is surface diffusion of vapor molecules adsorbed at the solid surface towards the droplet attached to it. This process is described by a free-boundary problem, which has been tackled in [21,22] in static and quasistatic approximations. In [23] generalization of this problem for more general boundary conditions was considered.

Nucleation of liquid droplets at a liquid-gas interface was considerably less studied. The important difference is the presence of the phase boundaries between three fluid phases characterized by three different contact angles and surface tensions. Nucleation from supersaturated water vapor on *n*-hexadecane was studied in [24], and the dependence of the critical supersaturation on temperature was determined.

In the present paper we consider certain aspects of the nucleation and growth of water droplets at a liquid-gas interface cooled by evaporation. Namely, we focus on two topics: (i) general analysis of the critical nucleation conditions in order to determine which type of nucleation—homogeneous or heterogeneous—is preferable and (ii) the droplet growth law in the presence of *two* growth mechanisms—diffusion flux from the vapor and surface diffusion flux at the interface, as well as in the presence of other drops. We solve this free-boundary problem numerically and compare the results with asymptotic solutions.

II. NUCLEATION OF DROPLETS

In this section we consider the nucleation of water droplets from a supersaturated vapor, near a liquid-gas interface cooled by evaporation. Two types of nucleation can occur: *homogeneous nucleation*, when the water nucleus appears in the gas phase near the interface, and *heterogeneous nucleation*, when the water nucleus is formed at the liquid-gas interface as a small liquid lens. In order to decide which nucleation type is more likely to occur, it is necessary to compare the corresponding free-energy nucleation barriers.

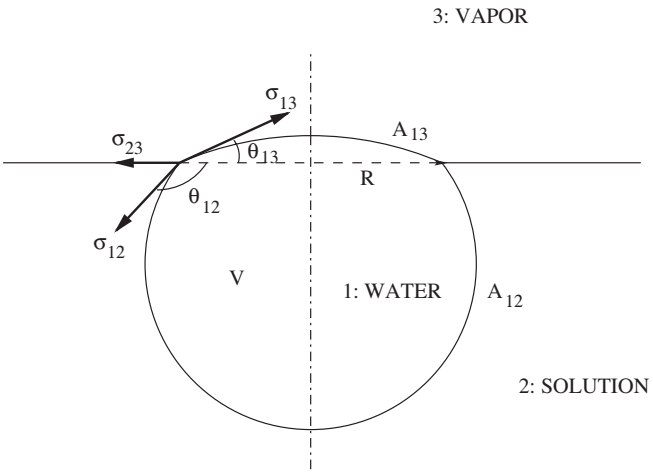

FIG. 1. Liquid droplet at a liquid-gas interface.

In the case of the homogeneous nucleation of a water droplet in the bulk of the vapor phase, the critical nucleation radius can be found from the standard expression for the nucleation work [25],

$$\Delta F^{hom}(R) = -(P' - P)V + \sigma_{13}A, \tag{1}$$

where P'-P is the pressure difference between the nucleus and the bulk phase, $V=4\pi R^3/3$ is the volume of the spherical nucleus with the radius R, $A=4\pi R^2$ is its surface area, and σ_{13} is the water-vapor interfacial tension (we refer to water, solution, and vapor phases as phases 1, 2, and 3, respectively). Equation (1) contains a negative volume contribution proportional to R^3 and a positive interfacial contribution proportional to R^2, and $\Delta F^{hom}(R)$ has a maximum at the critical nucleation radius $R=R_c^{hom}$, given by

$$R = R_c^{hom} = \frac{2\sigma_{13}}{P' - P}. \tag{2}$$

This critical nucleation radius determines the boundary between decaying fluctuations ($R<R_c$) and fluctuations leading to the formation of the new phase ($R>R_c$). The corresponding free-energy barrier is

$$\Delta F_c^{hom} = \frac{16\pi\sigma_{13}^3}{3(P' - P)^2} \tag{3}$$

(see [25]).

Now consider the nucleation of a water droplet at the gas-liquid interface (see Fig. 1). Such a droplet can exist under the condition of partial wetting, when the interfacial tensions σ_{ij} between the phases i and j, $i,j=1,2,3$, satisfy the relations $\sigma_{ij}<\sigma_{ik}+\sigma_{jk}$ for any i, j, k. The nucleation work is

$$\Delta F^{het} = -(P' - P)V + \sigma_{13}A_{13} + \sigma_{12}A_{12} - \sigma_{23}\pi R^2, \tag{4}$$

where A_{ij} are the interfacial areas between the phases i and j, and R is the radius of the three-phase contact line. The contact angles θ_{12} and θ_{13} are determined by the following relations [26]:

$$\cos\theta_{12} = \frac{\sigma_{23}^2 + \sigma_{12}^2 - \sigma_{13}^2}{2\sigma_{12}\sigma_{23}}, \quad \cos\theta_{13} = \frac{\sigma_{23}^2 + \sigma_{13}^2 - \sigma_{12}^2}{2\sigma_{13}\sigma_{23}}. \tag{5}$$

The volume of the droplet is given by

$$V = \frac{\pi}{3}R^3 A(\theta_{12}, \theta_{13}),$$

where

$$A(\theta_{12}, \theta_{13}) = \frac{\sin\theta_{12}(2 + \cos\theta_{12})}{(1 + \cos\theta_{12})^2} + \frac{\sin\theta_{13}(2 + \cos\theta_{13})}{(1 + \cos\theta_{13})^2}. \tag{6}$$

Using the expressions for the corresponding interfacial areas,

$$A_{12} = \frac{2\pi R^2}{1 + \cos\theta_{12}}, \quad A_{13} = \frac{2\pi R^2}{1 + \cos\theta_{13}},$$

and taking into account the stress balance equations

$$\sigma_{12}\sin\theta_{12} = \sigma_{13}\sin\theta_{13}, \quad \sigma_{23}\sin\theta_{13} = \sigma_{12}\sin(\theta_{12} + \theta_{13}) \tag{7}$$

(see Fig. 1), one finds the change ΔF_s in the interfacial part of the total free energy, determined by the last three terms on the right-hand side of Eq. (4), to be

$$\Delta F_s = \pi R^2 \sigma_{23} B(\theta_{12}, \theta_{13}).$$

Here,

$$B(\theta_{12}, \theta_{13}) = \frac{2\sin\theta_{12}}{(1 + \cos\theta_{13})\sin(\theta_{12} + \theta_{13})} + \frac{2\sin\theta_{13}}{(1 + \cos\theta_{12})\sin(\theta_{12} + \theta_{13})} - 1. \tag{8}$$

Thus, we obtain the following expression for the nucleation work:

$$\Delta F_R^{het} = -(P' - P)\frac{\pi}{3}R^3 A(\theta_{12}, \theta_{13}) + \pi R^2 \sigma_{23} B(\theta_{12}, \theta_{13}). \tag{9}$$

The critical nucleation radius in this case is

$$R_c^{het} = \frac{2\sigma_{23}}{P' - P}\frac{B(\theta_{12}, \theta_{13})}{A(\theta_{12}, \theta_{13})} = \frac{2\sigma_{23}}{P' - P}\frac{\sin\theta_{12}\sin\theta_{13}}{\sin(\theta_{12} + \theta_{13})}. \tag{10}$$

The corresponding free-energy barrier is

$$\Delta F_c^{het} = \frac{4\pi\sigma_{23}^3}{3(P'-P)^2}\frac{B^3(\theta_{12},\theta_{13})}{A^2(\theta_{12},\theta_{13})} = \frac{4\pi\sigma_{23}^3}{3(P'-P)^2}\frac{\sin^3\theta_{12}(2-3\cos\theta_{13}+\cos^3\theta_{13})+\sin^3\theta_{13}(2-3\cos\theta_{12}+\cos^3\theta_{12})}{\sin^3(\theta_{12}+\theta_{13})}. \quad (11)$$

The dependence of ΔF_c^{het} on the angles θ_{12} and θ_{13} is equivalent to that obtained in [24].

Using the notations

$$x = \tan\frac{\theta_{12}}{2}, \quad y = \tan\frac{\theta_{13}}{2},$$

trigonometric identities, as well as Eqs. (7), one can obtain the ratio $\Delta F_c^{het}/\Delta F_c^{hom}$ in the following simple form:

$$\frac{\Delta F_c^{het}}{\Delta F_c^{hom}} = \frac{y^3[x(3+x^2)+y(3+y^2)]}{(1+y^2)^3}. \quad (12)$$

It is easy to show that the ratio (12) is less than 1 for $xy<1$, which is equivalent to the inequality $\theta_{12}+\theta_{13}<\pi$. The latter is always satisfied since otherwise the stress balance at the contact line is not fulfilled (see Fig. 1).

Thus, we come to the conclusion that, under the conditions of partial wetting, the free-energy barrier of heterogeneous nucleation of a water droplet at a liquid-gas interface is lower than that of the homogeneous nucleation in the gas phase. Hence, it is more likely that the drops appear at the interface than in the bulk. Note, however, that this analysis ignores the possible presence of inhomogeneities and nucleation centers (like dust, for example) in the bulk and at the interface.

One can estimate the value of the critical nucleation radius (10). The pressure difference can be estimated as

$$P'-P = \frac{kT}{v_l}\ln\left(\frac{P}{P_{sat}}\right),$$

where v_l is the volume per molecule in the liquid phase, T is temperature, P_{sat} is the saturation pressure, and k is the Boltzmann constant [25,27]. For sufficiently small $\Delta P=P-P_{sat}$, the parameter $\ln(P/P_{sat})\sim\Delta P/P_{sat}$. The latter parameter is related to the temperature supersaturation parameter, $\Delta T/T_{sat}$, which can be more easily measured in experiment using the empirical correlation [19]

$$\frac{\Delta P}{P_{sat}} = \left(\frac{\Delta T}{T_{sat}}\right)^{0.8}.$$

In a typical experiment on the formation of a microporous polymer film, ΔT is between 3 K and 20 K, while T_{sat} is about 300 K, which gives $\Delta P/P_{sat}$ between 0.025 and 0.1. The volume per molecule for water, $v_l=M/\rho N$, where $M=18$ is the water molecular weight, $\rho=10^3$ kg/m^3 is the water density, and $N=6.023\times10^{23}$ is the Avogadro number. Assuming $\sigma_{23}\sim30$ mN/m and $B/A=0.75$, we find that the critical radius is between 6 nm and 25 nm. Thus, we conclude that the critical radius is rather small; however, the macroscopic approach is still valid.

Finally, let us discuss a possible effect of the *line tension* τ at the three-phase contact lines [28–31] on the above analysis of droplet nucleation. If the line tension is present, Eq. (4) for the nucleation work acquires an additional term on the right-hand side and becomes

$$\Delta F^{het} = -(P'-P)V+\sigma_{13}A_{13}+\sigma_{12}A_{12}-\sigma_{23}\pi R^2+\tau 2\pi R, \quad (13)$$

and the second of the stress balance conditions (7) changes to

$$(\sigma_{23}-\tau/R)\sin\theta_{13} = \sigma_{12}\sin(\theta_{12}+\theta_{13}). \quad (14)$$

Note that Eq. (14), as the condition for mechanical equilibrium, follows from the minimization (zero variation) of the sum of the surface and line energies. A typical value of τ in the case when no solid surface is present is about 10^{-12} N [32]. Taking a typical value of the interfacial tension $\sigma_{23}=30$ mN/m, we find that the line tension could be important only for a droplet with the radius $\tau/\sigma_{23}=0.3\times10^{-10}$ m, which is nonphysical. Hence, the effect of the line tension on the nucleation of water droplets at a liquid-gas interfaces can be neglected.

III. DROPLET GROWTH

In this section we consider the growth of a water droplet that has nucleated at a liquid-gas interface from the saturated vapor due to the interface evaporative cooling and has formed a liquid lens shown in Fig. 1; at the interface, the region occupied by part of the water droplet in contact with the gas is a circle with the radius R^*. We assume that the droplet grows by means of the following two mechanisms: attachment of water molecules directly from the humid gas and attachment of water molecules adsorbed at the liquid-gas interface from the vapor; thus, the radius R^* is an increasing function of time, t^*.

In a typical experiment, a humid gas moves with a certain speed U along the liquid-gas interface. Assuming that the gas flow forms a laminar boundary layer with the characteristic thickness δ, one can estimate the flux of water molecules j from the gas phase to the interface using the following formula for the Sherwood number [33,34]:

$$\mathrm{Sh} = j\delta/D_0c_0 \sim \mathrm{Re}^{1/2}\mathrm{Sc}^{1/2}, \quad (15)$$

where c_0 is the concentration of water vapor at the edge of the boundary layer, D_0 is the bulk diffusion coefficient of water molecules in the gas phase, $\mathrm{Re}=U\delta/\nu$ is the Reynolds number (ν is the kinematic viscosity of the gas), and $\mathrm{Sc}=\nu/D_0$ is the Schmidt number. Note, however, that Eq. (15) is valid if the vapor flux at the liquid-gas interface is determined by diffusion from the gas phase and all water molecules coming to the interface are adsorbed at it. This may not be true since the adsorbed water molecules will block the interface sites for the adsorption of other molecules. This

effect of adsorption saturation can be described by multiplying the diffusion flux by the fraction of the surface free for adsorption; thus, one obtains $j=j_s(1-c^*/c_s^*)$, where j_s is the saturated maximal flux which is determined by the interface cooling caused by the solvent evaporation. Water molecules adsorbed at the liquid-gas interface can lead to another effect: they can block the solvent evaporation and reduce the evaporation rate. This will decrease the evaporative cooling rate, increase the interfacial temperature and the equilibrium concentration of water vapor, which, in turn, will decrease the saturated diffusion flux j_s. This effect can be accounted for by assuming that $j_s \sim (1-c^*/c_s^*)$; thus, in this case $j \sim (1-c^*/c_s^*)^2$. Note also that due to a nonlinear dependence of the vapor equilibrium concentration on temperature, the dependence of j_s on the decrease of the cooling rate proportional to $(1-c^*/c_s^*)$ may be more complicated and involve some nontrivial exponents. Therefore, in the present paper, we describe the effect of water molecules adsorbed at the liquid-gas interface phenomenologically and consider the flux j to be a function of the surface concentration of water molecules, c^*, in the form

$$j = j_s(1 - c^*/c_s^*)^s, \tag{16}$$

where c_s^* is the saturation concentration, s is the saturation exponent, and j_s is the maximal flux that depends on the characteristics of the diffusion and thermal boundary layer at the interface in the gas phase, interfacial temperature, vapor saturation conditions, etc. Equation (16) with $s=0$ corresponds to the nonsaturated vapor adsorption at the liquid-gas interface, controlled by diffusion and described by Eq. (15) with $j=j_0$.

Thus, we shall consider two cases: (i) unsaturated condensation, with the vapor flux described by (16) with $s=0$ and (ii) saturated condensation, corresponding to Eq. (16) with $s>0$.

A. Unsaturated condensation

In this subsection we consider the growth of a liquid droplet nucleated at a liquid-gas interface when the vapor diffusion flux from the gas phase does not depend on the surface concentration of water molecules. We also assume that the vapor fluxes at the liquid-gas interface and at the droplet-gas interface are given by the same constant value, j_0. The system configuration is shown in Fig. 2.

Diffusion of water molecules adsorbed at the liquid-gas interface around the droplet, in the presence of similar droplets nucleated at the interface, can be modeled by the following radially-symmetric free-boundary problem for the surface concentration of water molecules, $c^*(r^*,t^*)$, and the droplet radius $R^*(t^*)$:

$$\frac{\partial c^*}{\partial t^*} = \frac{D}{r^*}\frac{\partial}{\partial r^*}\left(r^*\frac{\partial c^*}{\partial r^*}\right) + j_0, \quad R^*(t^*) < r^* < R_b^*, \tag{17}$$

where the radial coordinate r^* is measured from the droplet center at the interface, D is the surface diffusivity of the adsorbed water molecules, and R_b^* is the size of the "basin" at the interface from which the drop collects water molecules,

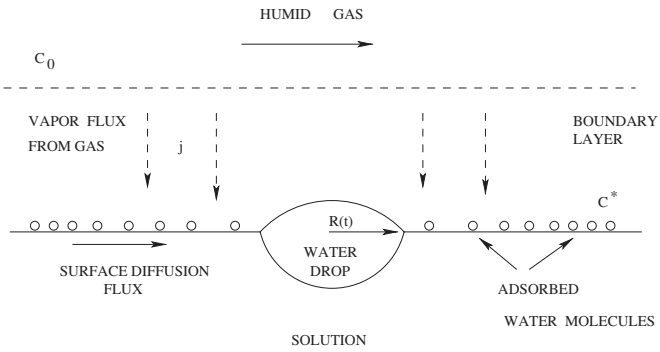

FIG. 2. A water droplet at a liquid-gas interface growing by diffusion of vapor from the gas and surface diffusion of adsorbed water molecules.

so that $2R_b^*$ is the average distance between the different water droplets nucleated at the interface. We assume a complete absorption of water molecules at the droplet boundary, $r^*=R^*$,

$$c^*(R^*(t^*),t^*) = 0, \tag{18}$$

and the no-flux condition at the boundary of the "basin,"

$$\left.\frac{\partial c^*}{\partial r^*}\right|_{r^*=R_b^*} = 0. \tag{19}$$

The droplet growth is governed by the mass balance equation

$$\frac{\lambda}{V_0}(R^*)^2\frac{dR^*}{dt^*} = 2\pi R^* D \left.\frac{\partial c^*}{\partial r^*}\right|_{r^*=R^*(t^*)} + j_0\pi(R^*)^2, \tag{20}$$

where V_0 is the volume per one molecule in the water and λ is the geometric factor that determines the relation between the droplet volume V^* and the "interfacial radius" R^*, $V^*=(R^*)^3\lambda/3$. Since the nucleation time and the critical nucleation radius are negligible in comparison with the characteristic time of the droplet growth and the characteristic droplet size, respectively, the following initial conditions can be used:

$$c^*(r^*,0) = 0 (0 < r^* < R_b^*), \quad R^*(0) = 0. \tag{21}$$

Using the dimensionless variables

$$t = \frac{t^*}{t_0}, \quad c = \frac{c^*}{c_0}, \quad r = \frac{r^*}{r_0}, \quad R = \frac{R^*}{r_0}, \quad R_b = \frac{R_b^*}{r_0},$$

with the reference quantities

$$t_0 = \frac{\lambda^2 D}{\pi^2 j_0^2 V_0^2}, \quad c_0 = \frac{\lambda^2 D}{\pi^2 j_0 V_0^2}, \quad r_0 = \frac{\lambda D}{\pi j_0 V_0},$$

one can write the problem (17)–(21) in the following form:

$$\frac{\partial c}{\partial t} = \frac{1}{r}\frac{\partial}{\partial r}\left(r\frac{\partial c}{\partial r}\right) + 1, \quad R(t) < r < R_b, \quad t > 0, \tag{22}$$

$$R^2\frac{dR}{dt} = 2R\left.\frac{\partial c}{\partial r}\right|_{r=R(t)} + R^2, \quad t > 0, \tag{23}$$

$$r = R(t): \quad c = 0; \quad r = R_b: \quad \frac{\partial c}{\partial r} = 0; \quad c(r,0) = 0; \quad R(0) = 0. \tag{24}$$

First, we shall consider two analytically tractable limiting cases: (i) $R_b \gg 1$ (a sparse system of nuclei or large mass flux) and (ii) $R_b \ll 1$ (a dense system of nuclei or small mass flux).

1. The case $R_b \gg 1$

Consider the limit $R_b \to \infty$ in Eqs. (24), which corresponds to a sparse system of nucleated droplets or large mass flux onto a separate droplet. In this case it is convenient to reformulate the problem (22)–(24) in terms of integral equations. Consider an auxiliary problem

$$\frac{\partial c}{\partial t} = \nabla^2 c + 1 - J_-(t)\,\delta(x,y), \tag{25}$$

which will be solved in the entire plane $-\infty < x,y < \infty$, with the initial condition $c=0$ at $t=0$. Here $\delta(x,y)$ is the Dirac delta function, so that the last term in Eq. (25) represents a localized sink at the origin with as yet unknown strength. We look for $J_-(t)$ and $R(t)$ such that the conditions (23) and (24) are satisfied. Then for $r > R(t)$ the problems (22)–(24) and (25), (23), and (24) are equivalent. Solution of Eq. (25) with the zero initial condition can be written as

$$c(r,t) = t - \frac{1}{4\pi}\int_0^t \frac{1}{\tau}\exp\left(-\frac{r^2}{4\tau}\right) J_-(t-\tau)\,d\tau. \tag{26}$$

Using the conditions (23) and (24) one obtains the following system of two equations for the two unknowns $R(t)$ and $J_-(t)$:

$$t = \frac{1}{4\pi}\int_0^t \frac{1}{\tau}\exp\left(-\frac{R^2(t)}{4\tau}\right) J_-(t-\tau)\,d\tau, \tag{27}$$

$$\frac{dR}{dt} = \frac{1}{4\pi}\int_0^t \frac{1}{\tau^2}\exp\left(-\frac{R^2(t)}{4\tau}\right) J_-(t-\tau)\,d\tau + 1. \tag{28}$$

The substitution $\tau = t/y$ transforms Eqs. (27) and (28) into

$$t = \frac{1}{4\pi}\int_1^\infty \frac{1}{y}\exp\left(-\frac{R^2(t)}{4t}y\right) J_-\left(t - \frac{t}{y}\right) dy, \tag{29}$$

$$\frac{dR}{dt} = \frac{1}{4\pi t}\int_1^\infty \exp\left(-\frac{R^2(t)}{4t}y\right) J_-\left(t - \frac{t}{y}\right) dy + 1. \tag{30}$$

Now we can derive approximate solutions of the integral equations (29) and (30) for the limiting cases of small and large times.

First we consider the case $t \ll 1$. We assume that, for $t \ll 1$,

$$\frac{R^2(t)}{4t} \ll 1. \tag{31}$$

This assumption can be verified *a posteriori* when the solution of the problem is found. Under this assumption the integrals in Eqs. (29) and (30) can be asymptotically evaluated. Consider, for example, the integral in Eq. (30). Making a substitution

$$z = \frac{R^2(t)}{4t}y \equiv \mu y,$$

we obtain

$$\begin{aligned}\int_1^\infty \exp\left(-\frac{R^2(t)}{4t}y\right) J_-\left(t - \frac{t}{y}\right) dy &= \mu\int_\mu^\infty e^{-z} J_-(t - \mu t/z)\,dz \\ &\sim \mu\int_\mu^\infty e^{-z} J_-(t)\,dz \sim \mu J_-(t) = \frac{R^2(t)}{4t} J_-(t).\end{aligned} \tag{32}$$

In a similar way, the integral in Eq. (29) can be asymptotically evaluated as

$$\int_1^\infty \frac{1}{y}\exp\left(-\frac{R^2(t)}{4t}y\right) J_-\left(t - \frac{t}{y}\right) dy \sim J_-(t)\ln\frac{4t}{R^2}. \tag{33}$$

Substituting Eqs. (32) and (33) into Eqs. (29) and (30) and eliminating $J_-(t)$ yields the following differential equation for $R(t)$:

$$\frac{dR}{dt} = \frac{4t}{R^2\ln(4t/R^2)}, \quad R(0) = 0. \tag{34}$$

The change of variables

$$R(t) = [36t^2 w(\tau)]^{1/3}, \quad \tau = -\ln t,$$

reduces Eq. (34) to

$$\frac{dw}{d\tau} = 2w - \frac{1}{\tau + 2\ln 2/(9w)}, \quad w(\infty) = 0.$$

Neglecting the logarithmic term for large τ, one finds

$$w(\tau) = e^{2\tau}\int_\tau^\infty \frac{1}{s}e^{-2s}ds \sim \frac{1}{2\tau} \quad (\tau \gg 1).$$

Finally,

$$R(t) \sim \left(\frac{18t^2}{\ln\dfrac{1}{t}}\right)^{1/3}. \tag{35}$$

Now we consider the case $t \gg 1$. We assume that in this limit $R^2(t)/4t \gg 1$, which can be verified *a posteriori*. In this case, Eq. (29) is satisfied by the ansatz

$$R(t) = vt, \quad J_-(t) = at^b e^{v^2 t}, \tag{36}$$

with

$$a = 8\sqrt{\pi}v, \quad b = 3/2. \tag{37}$$

Substituting Eqs. (36) and (37) into Eq. (30) one finds $v=3$. Thus, for $t \gg 1$, the droplet radius $R(t) \sim 3t$.

The concentration profile $c(r,t)$ can also be determined from the integral equations. It is easier, however, to determine the concentration directly from Eqs. (22)–(24). In order to do it we make a coordinate transformation

$$x = r/R(t),$$

so that the moving free-boundary problem (22)–(24) reduces to a problem over a time-independent spatial region $x>1$:

$$\frac{\partial c}{\partial t} - x\frac{1}{R}\frac{dR}{dt}\frac{\partial c}{\partial x} = \frac{1}{R^2}\frac{1}{x}\frac{\partial}{\partial x}\left(x\frac{\partial c}{\partial x}\right) + 1, \quad x>1, \quad t>0, \tag{38}$$

$$\frac{dR}{dt} = \left.\frac{2}{R^2}\frac{\partial c}{\partial x}\right|_{x=1} + 1, \quad t>0, \tag{39}$$

$$x=1: \quad c=0; \quad x=\infty: \quad \frac{\partial c}{\partial x}=0; \quad c(x,0)=0; \quad R(0)=0. \tag{40}$$

Note that we consider here $R_b=\infty$ and retain the same notation $c(x,t)$ for the unknown concentration as used before when the concentration was a function of r and t.

We consider the long-time behavior of the solution. Thus, we introduce a small parameter ϵ and scale the time t as $t=\tau/\epsilon$, where τ is an $O(1)$ quantity. We also rescale the other variables in the problem as

$$x = 1+\epsilon\xi, \quad c(x,t) = \frac{1}{\epsilon}a(\xi,\tau), \quad R(t) = \frac{1}{\epsilon}\rho(\tau).$$

Equation (38) takes the form

$$\frac{\partial a}{\partial \tau} - \frac{1}{\epsilon}(1+\epsilon\xi)\frac{1}{\rho}\frac{d\rho}{d\tau}\frac{\partial a}{\partial \xi} = \frac{1}{\epsilon}\frac{1}{\rho^2}\frac{1}{1+\epsilon\xi}\frac{\partial}{\partial \xi}\left[(1+\epsilon\xi)\frac{\partial a}{\partial \xi}\right] + 1, \tag{41}$$

$$\xi>0, \quad \tau>0.$$

Equation (41) reduces at the leading order in $\epsilon \ll 1$ to

$$-\frac{1}{\rho}\frac{d\rho}{d\tau}\frac{\partial a}{\partial \xi} = \frac{1}{\rho^2}\frac{\partial^2 a}{\partial \xi^2}, \quad \xi>0. \tag{42}$$

The boundary conditions are

$$a(0,\tau)=0, \quad a(\infty,\tau)=\tau. \tag{43}$$

The second boundary condition is due to the fact that because of the presence of the unit source term in Eq. (38),

$$c(\infty,t)=t.$$

The solution of Eqs. (42) and (43) is

$$a(\xi,\tau) = \tau\left[1-\exp\left(-\rho\frac{d\rho}{d\tau}\xi\right)\right].$$

Thus, for large t,

$$c(x,t) = t\left[1-\exp\left(-R\frac{dR}{dt}(x-1)\right)\right], \tag{44}$$

so that

$$\left.\frac{\partial c}{\partial x}\right|_{x=1} = tR\frac{dR}{dt},$$

and the equation for the droplet radius takes the form

$$\frac{dR}{dt} = \frac{2t}{R}\frac{dR}{dt} + 1. \tag{45}$$

An implicit form solution of Eq. (45) is

$$R^2(3t-R) = \text{const}.$$

For large t,

$$R(t) \approx 3t,$$

in agreement with the result obtained with the use of integral equations.

The long-time solution (44) can be written in terms of the original variables as

$$c(r,t) \sim t\left[1-\exp\left(-\frac{dR}{dt}[r-R(t)]\right)\right] \quad (r>3t), \tag{46}$$

and for $R=3t$ it reduces to

$$c(r,t) \sim t\{1-\exp[-3(r-3t)]\} \quad (r>3t). \tag{47}$$

We have verified the accuracy of the obtained approximate asymptotic solutions by solving the problem (22)–(24) numerically by means of a finite-difference method with central differences in space, the Crank-Nicholson time-integration scheme for the concentration field, and with the predictor-corrector approach for $R(t)$ in which the radius of the droplet was updated at the predictor step and the updated radius was used at the corrector step. The results of the numerical computations up to $t=10$ are shown in Figs. 3 and 4; they demonstrate the accuracy of the approximate solution.

Accidentally, the analytical solution obtained for $t \gg 1$ provides a reasonably good approximation to the numerical solution not only for $t \gg 1$ but also for $t=O(1)$. This is illustrated by Fig. 5, where the concentration profiles are compared at time $t=1$.

We finally conclude that in the case $R_b \gg 1$ the droplet radius grows according to the law (35) at the early stage of the process and with a constant speed at later stages.

2. The case $R_b \ll 1$

Now consider the case $R_b \ll 1$, which corresponds to a dense system of nucleated droplets at the liquid-gas interface or a small mass flux onto a separate droplet. In this case it is convenient to make the coordinate transformation

$$x = \frac{r}{R(t)},$$

so that the moving boundary of the droplet would become stationary. Using the new variable, the problem (22)–(24) can be written as

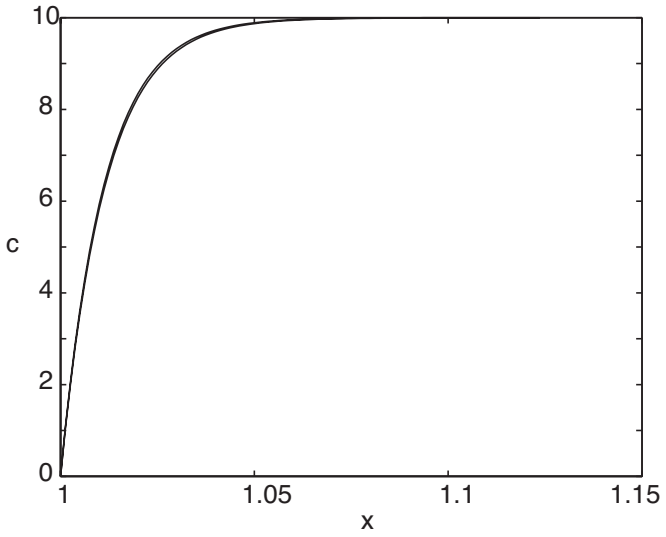

FIG. 3. Numerical and analytical solutions of the problem (22)–(24). Profiles of the concentration c as a function of the spatial variable $x=r/R(t)$ at time $t=10$; numerical and analytical solutions are almost indistinguishable.

$$\frac{\partial c}{\partial t} - x\frac{1}{R}\frac{dR}{dt}\frac{\partial c}{\partial x} = \frac{1}{R^2}\frac{1}{x}\frac{\partial}{\partial x}\left(x\frac{\partial c}{\partial x}\right) + 1, \quad 1 < x < \frac{R_b}{R(t)}, \quad t > 0, \tag{48}$$

$$\frac{dR}{dt} = \left.\frac{2}{R^2}\frac{\partial c}{\partial x}\right|_{x=1} + 1, \quad t > 0, \tag{49}$$

$$x = 1: \quad c = 0; \quad x = \frac{R_b}{R}: \quad \frac{\partial c}{\partial x} = 0; \quad c(x,0) = 0; \quad R(0) = 0. \tag{50}$$

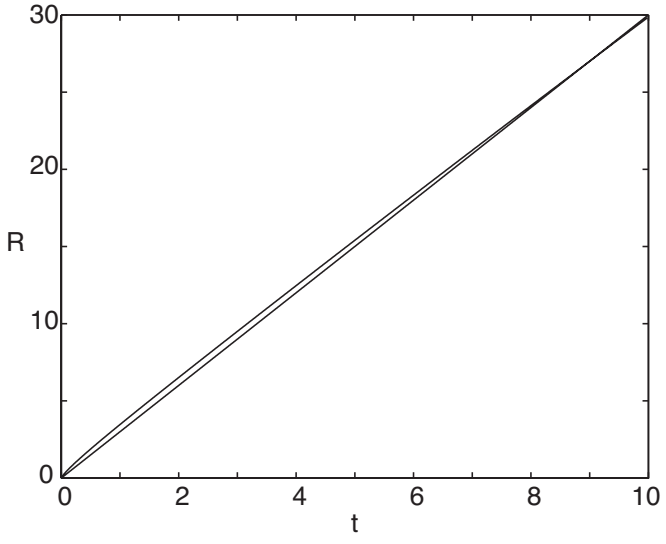

FIG. 4. Numerical and analytical solutions of the problem (22)–(24). The dependence of the radius R on time t, $0<t<10$; the analytical solution provides a good approximation to the numerical solution for almost all times (except for t small); the upper curve is the numerical solution.

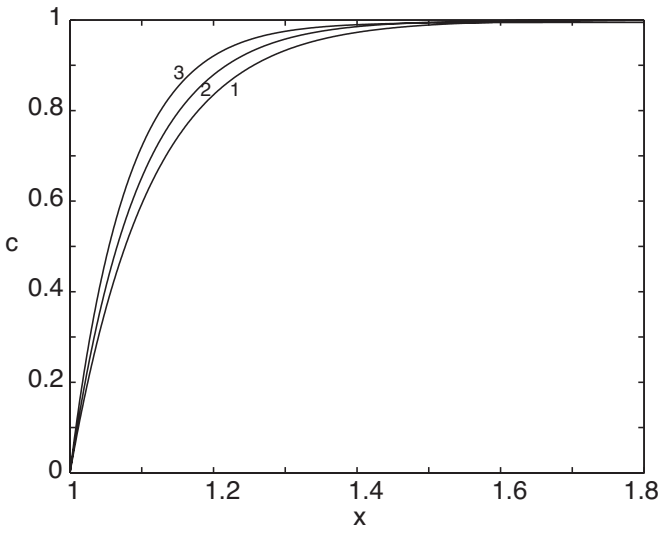

FIG. 5. Numerical and analytical solutions of the problem (22)–(24) at time $t=1$. The figure displays profiles of the concentration c as a function of the spatial variable $x=r/R(t)$. Curve (1), analytical solution (47); curve (2), analytical solution (46) with numerically determined $R=3.4$ and $dR/dt=3.1$ (at time $t=1$); curve (3), numerical solution.

Rescaling the variables, $c=R_b^2 C$, $R=R_b\rho$, and $t=R_b\tau$, we obtain

$$R_b\frac{\partial C}{\partial \tau} - R_b^2\frac{x}{\rho}\frac{d\rho}{d\tau}\frac{\partial C}{\partial x} = \frac{1}{\rho^2}\frac{1}{x}\frac{\partial}{\partial x}\left(x\frac{\partial C}{\partial x}\right) + 1, \quad 1 < x < \frac{1}{\rho}, \quad t > 0,$$

$$\frac{d\rho}{d\tau} = \left.\frac{2}{\rho^2}\frac{\partial C}{\partial x}\right|_{x=1} + 1, \quad t > 0,$$

$$x = 1: \quad C = 0; \quad x = \frac{1}{\rho}: \quad \frac{\partial C}{\partial x} = 0; \quad C(x,0) = 0; \quad \rho(0) = 0. \tag{51}$$

For $R_b \ll 1$, after a short transient period of the order $\tau \sim R_b$, the solution of the initial value problem (51) tends to the solution of the leading-order stationary problem which is given by

$$C = \frac{1}{2}\ln x + \frac{\rho^2}{4}(1 - x^2). \tag{52}$$

Substituting Eq. (52) into Eqs. (51), one obtains $d\rho/d\tau = \rho^{-2}$, so that $\rho \sim (3\tau)^{1/3}$ and

$$R \sim (3R_b^2 t)^{1/3} \tag{53}$$

or, in dimensional quantities,

$$R^* \sim [3(R_b^*)^2 r_0 t^*/t_0]^{1/3}.$$

Figure 6 compares the approximate solution with a numerical solution of Eqs. (22)–(24). One can see that, at the initial stage of growth, the difference between the numerical solu-

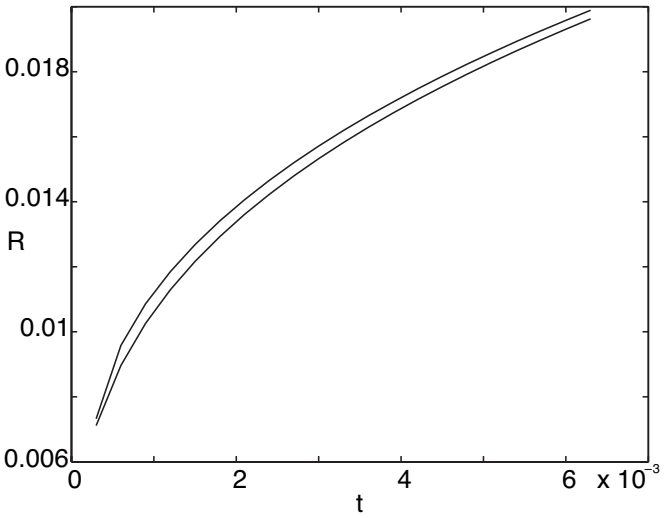

FIG. 6. Dependence of the droplet radius R on time t. Here $R_b=0.02$. The upper curve is the numerical solution of the problem (22)–(24). The lower curve is the analytic solution (53).

tion of the full problem and the asymptotic solution is about 5%.

B. Saturated condensation

We now consider the case when vapor condensation at the liquid-gas interface depends on the interfacial concentration of water molecules so that the vapor flux to the interface from the gas phase is given by Eq. (16) with $s>0$. We assume here that the vapor is condensing only at the interface between the gas and solution, but it is not condensing at the droplet-gas interface, since the latter is not cooled by the solvent evaporation. Note that this effect is *not* accounted for by Eq. (16): this equation determines the dependence of the vapor diffusion flux from the gas on the concentration of water molecules adsorbed *around* the droplet sitting at the liquid-gas interface (see Fig. 1) and growing only due to the *surface diffusion* of the adsorbed water molecules (see Fig. 2). Also, here we shall study the growth of a single droplet in an infinite domain—i.e., in the absence of other droplets. Thus, we consider the following problem for the surface concentration of water molecules, c^*,

$$\frac{\partial c^*}{\partial t^*}=\frac{D}{r^*}\frac{\partial}{\partial r^*}\left(r^*\frac{\partial c^*}{\partial r^*}\right)+j_s(1-c^*/c_s^*)^s,\quad R^*(t^*)<r^*, \tag{54}$$

$$c^*(R^*(t^*),t^*)=0,\qquad \left.\frac{\partial c^*}{\partial r^*}\right|_{r^*=\infty}=0, \tag{55}$$

$$\frac{\lambda}{V_0}(R^*)^2\frac{dR^*}{dt^*}=2\pi R^* D\left.\frac{\partial c^*}{\partial r^*}\right|_{r^*=R^*(t^*)}, \tag{56}$$

$$c^*(r^*,0)=0\ (r^*>0),\quad R^*(0)=0. \tag{57}$$

We introduce the dimensionless variables

$$t=\frac{t^*}{t_0},\quad c=\frac{c^*}{c_0},\quad c_s=\frac{c_s^*}{c_0},\quad r=\frac{r^*}{r_0},\quad R=\frac{R^*}{r_0},$$

with the reference quantities

$$c_0=\frac{\lambda^2 D}{\pi^2 j_s V_0^2},\quad t_0=\frac{c_0}{j_s},\quad r_0=\sqrt{Dt_0},$$

to obtain the following dimensionless problem:

$$\frac{\partial c}{\partial t}=\frac{1}{r}\frac{\partial}{\partial r}\left(r\frac{\partial c}{\partial r}\right)+(1-c/c_s)^s,\quad R(t)<r,\quad t>0, \tag{58}$$

$$R^2\frac{dR}{dt}=2R\left.\frac{\partial c}{\partial r}\right|_{r=R(t)},\quad t>0, \tag{59}$$

$$r=R(t):\quad c=0;\quad r=\infty:\quad \frac{\partial c}{\partial r}=0,\quad c(r,0)=0,\quad R(0)=0. \tag{60}$$

Below we compare three particular cases corresponding to three different values of the saturation exponent s: no saturation, $s=0$; linear saturation, $s=1$; and oversaturation, $s\gg 1$. In each case we determine the droplet growth law for large times, $t\gg 1$.

The no-saturation case, $s=0$, is similar to that discussed in the previous subsection; the only difference between the problems (22)–(24) and (58)–(60) is the absence of the condensation source term in Eq. (59). Thus, instead of Eq. (45) we obtain

$$\frac{dR}{dt}=\frac{2t}{R}\frac{dR}{dt},$$

yielding the linear asymptotic law of the droplet growth,

$$R(t)\sim 2t.$$

In the linear saturation case $s=1$, it is convenient to make the coordinate transformation, $x=r/R(t)$, which reduces the problem to

$$\frac{\partial c}{\partial t}-x\frac{1}{R}\frac{dR}{dt}\frac{\partial c}{\partial x}=\frac{1}{R^2}\frac{1}{x}\frac{\partial}{\partial x}\left(x\frac{\partial c}{\partial x}\right)+1-\frac{c}{c_s},\quad x>1,\quad t>0, \tag{61}$$

$$\frac{dR}{dt}=\left.\frac{2}{R^2}\frac{\partial c}{\partial x}\right|_{x=1},\quad t>0, \tag{62}$$

$$x=1:\quad c=0;\quad x=\infty:\quad \frac{\partial c}{\partial x}=0,\quad c(x,0)=0,\quad R(0)=0. \tag{63}$$

For $t\gg 1$ we rescale the variables as

$$t=\frac{\tau}{\epsilon},\quad x=1+\sqrt{\epsilon}\xi,\quad c(x,t)=a(\xi,\tau),\quad R(t)=\frac{1}{\sqrt{\epsilon}}\rho(\tau),$$

to obtain, at the leading order in $\epsilon\ll 1$,

$$\frac{1}{\rho^2}\frac{\partial^2 a}{\partial \xi^2} + 1 - \frac{a}{c_s} = 0, \quad a(0,\tau) = 0, \quad \left.\frac{\partial a}{\partial \xi}\right|_{\xi=\infty} = 0,$$

$$\frac{d\rho}{d\tau} = \frac{2}{\rho^2}\left.\frac{\partial a}{\partial \xi}\right|_{\xi=0}.$$

The solution of this problem is given by

$$a = c_s - \exp(-\rho\xi/\sqrt{c_s}), \quad \rho = \frac{2}{c_s^{1/4}}\sqrt{\tau}.$$

Thus, in the linear saturation case the radius of the droplet grows for large times as

$$R(t) \sim \frac{2}{c_s^{1/4}}\sqrt{t}.$$

The oversaturated case $s \to \infty$ is described by the following problem:

$$\frac{\partial c}{\partial t} = \frac{1}{r}\frac{\partial}{\partial r}\left(r\frac{\partial c}{\partial r}\right), \quad r > R(t), \quad t > 0, \tag{64}$$

$$R^2\frac{dR}{dt} = 2R\left.\frac{\partial c}{\partial r}\right|_{r=R(t)}, \quad t > 0, \tag{65}$$

$$r = R(t): \quad c = 0; \quad r = \infty: \quad c = c_s, \quad c(r,0) = 0, \quad R(0) = 0. \tag{66}$$

For $t \gg 1$ one has $R(t) \gg 1$, and Eq. (64) can be replaced by

$$\frac{\partial c}{\partial t} = \frac{\partial^2 c}{\partial r^2}, \quad r > R(t), \quad t > 0. \tag{67}$$

The problem (65)–(67) has the following self-similar solution:

$$c(r,t) = c_s \operatorname{erf}\left(\frac{r - R(t)}{2\sqrt{t}}\right). \tag{68}$$

Substituting Eq. (68) into Eq. (65) and solving the resulting equation yields

$$R(t) = \left(\frac{8c_s}{\sqrt{\pi}}\right)^{1/2} t^{1/4}.$$

We observe that the growth law of the droplet depends on the saturation exponent s, $R(t) \propto t^{\alpha_s}$, with $\alpha_0 = 1$, $\alpha_1 = 1/2$, and $\alpha_\infty = 1/4$. Based on these three results, one can suggest the following interpolation formula for the growth exponent α_s:

$$\alpha_s = \frac{2+s}{2+4s}.$$

The growth exponent $\alpha_1 = 1/2$ differs from those predicted by previous theories [17–23].

IV. CONCLUSIONS

We have studied the nucleation and growth of liquid droplets at a liquid-gas interface cooled by evaporation. We have shown that the ratio of the nucleation barriers for homogeneous and heterogeneous nucleations depends only on the contact angles that characterize the droplet shape (liquid lens) nucleated at the liquid-gas interface. Analyzing this dependence we have concluded that heterogeneous nucleation is always more likely to occur than the homogeneous one.

We have studied the growth of a droplet nucleated at a liquid-gas interface in the case when the growth is caused by the combination of two mechanisms: diffusion flux from the vapor phase onto the part of the droplet surface resting above the liquid and surface diffusion flux of molecules adsorbed at the liquid-gas interface onto the droplet interface boundary. We have considered two cases, depending on whether the diffusion flux from the vapor phase, j, depends on the surface concentration c^* of the adsorbed water molecules: unsaturated condensation, when j does not depend on c^*, and saturated condensation, when j depends on c^* according to Eq. (16).

We have shown that the droplet growth caused by these two mechanisms can be described by a free-boundary problem, and we have solved this problem numerically and analyzed the solutions asymptotically in various limits. As a result, we have found the exponents of the growth power law at different stages of the droplet growth. In the unsaturated condensation case, we have found that the growth law depends not only on the growth stage (small or large time) but also on the presence of other drops—namely, whether the system of drops nucleated at the interface is sparse or dense. We have shown that for a sparse system of drops the drop radius grows initially as $[t^2/\ln(1/t)]^{1/3}$. This growth law is different from those obtained previously in the static and quasistatic approximations. We have also shown that at the later stages in this limit the droplet radius grows linearly in time. However, this crossover does not involve the droplet coalescence, it follows just from the properties of the free-boundary problem. At the very late stages, when the drops grew into a dense system, the growth law exhibits the second crossover, to a slower growth rate $\sim t^{1/3}$. In the case of saturated condensation, our investigation of the growth of a single droplet shows that the growth exponent depends on the degree of saturation. In particular, in the case of linear saturation given by $s = 1$ in Eq. (16), we have shown that the late stage growth exponent is 1/2. It would be interesting to verify this conclusion in experiments.

ACKNOWLEDGMENT

This work was supported by U.S. DOE Grant No. DE-FG02-03ER46069.

[1] G. Widawski, M. Rawiso, and B. Francois, Nature (London) **369**, 387 (1994).
[2] B. Francois, O. Pitois, and J. Francois, Adv. Mater. (Weinheim, Ger.) **7**, 1041 (1995).
[3] N. Maruyama, T. Koito, J. Nishida, T. Sawadaishi, X. Cieren, K. Ijiro, O. Karthaus, and M. Shimomura, Thin Solid Films **327–329**, 854 (1998).
[4] O. Pitois and B. Francois, Eur. Phys. J. B **8**, 225 (1999).
[5] B. de Boer, U. Stalmach, H. Nijland, and G. Hadziioannou, Adv. Mater. (Weinheim, Ger.) **12**, 1581 (2000).
[6] T. Nishikawa, J. Nishida, R. Ookura, S.-I. Nishimura, S. Wada, T. Karino, and M. Shimomura, Mater. Sci. Eng., C **10**, 141 (1999).
[7] T. Nishikawa, J. Nishida, R. Ookura, S.-I. Nishimura, S. Wada, T. Karino, and M. Shimomura, Mater. Sci. Eng., C **8–9**, 495 (1999).
[8] O. Karthaus, N. Maruyama, X. Cieren, M. Shinomura, H. Hasegawa, and T. Hashimoto, Langmuir **16**, 6071 (2000).
[9] M. Srinivasarao, D. Collings, A. Philips, and S. Patel, Science **292**, 79 (2001).
[10] J. Peng, Y. Han, and Y. Yang, Polymer **45**, 447 (2004).
[11] B. Erdogan, L. L. Song, J. N. Wilson, J. O. Park, M. Srinivasarao, and U. H. F. Bunz, J. Am. Chem. Soc. **126**, 3678 (2004).
[12] E. Bormashenko, R. Pogreb, O. Stanevsky, Y. Bormashenko, and O. Gendelman, Mater. Lett. **59**, 3553 (2005).
[13] M. Tanaka, M. Takebayashi, M. Miyama, J. Nishida, and M. Shimomura, Biomed. Mater. Eng. **14**, 439 (2004).
[14] M. Imada, S. Noda, A. Chutinan, T. Tokuda, M. Murata, and G. Sasaki, Appl. Phys. Lett. **75**, 316 (1999).
[15] Y. P. Rakovich, J. F. Donegan, M. Gerlach, A. L. Bradley, T. M. Connolly, J. J. Boland, N. Gaponik, and A. Rogach, Phys. Rev. A **70**, 051801(R) (2004).
[16] M. Haupt, S. Miller, R. Sauer, and K. Thonke, J. Appl. Phys. **96**, 3065 (2004).
[17] F. Family and P. Meakin, Phys. Rev. Lett. **61**, 428 (1988).
[18] D. Fritter, C. M. Knobler, and D. A. Beysens, Phys. Rev. A **43**, 2858 (1991).
[19] D. Beysens, A. Steyer, P. Guenon, D. Fritter, and C. M. Knobler, Phase Transitions **31**, 219 (1991).
[20] P. Meakin, Rep. Prog. Phys. **55**, 157 (1992).
[21] A. Steyer, P. Guenoun, D. Beysens, and C. M. Knobler, Phys. Rev. A **44**, 8271 (1991).
[22] P. L. Krapivsky, Phys. Rev. E **47**, 1199 (1993).
[23] Z. Tavassoli and G. J. Rodgers, Eur. Phys. J. B **14**, 139 (2000).
[24] A. D. Alexandrov, B. V. Toshev, and A. D. Scheludko, Langmuir **7**, 3211 (1991).
[25] L. D. Landau and E. M. Lifshitz, *Statistical Physics* (Pergamon, Oxford, 1980).
[26] H. M. Princen, in *Surface and Colloid Science*, edited by E. Matijevic (Wiley-Interscience, New York, 1976), Vol. 2.
[27] J. Frenkel, *Kinetic Theory of Liquids* (Dover, New York, 1955).
[28] J. S. Rowlinson and B. Widom, *Molecular Theory of Capillarity* (Clarendon Press, Oxford, 1982).
[29] B. Widom, Mol. Phys. **96**, 1019 (1999).
[30] A. Marmur, J. Colloid Interface Sci. **186**, 462 (1997).
[31] A. Marmur, Colloids Surf., A **136**, 81 (1998).
[32] A. Checco, P. Guenoun, and J. Daillant, Phys. Rev. Lett. **91**, 186101 (2003).
[33] V. G. Levich, *Physicochemical Hydrodynamics* (Prentice-Hall, Englewood Cliffs, NJ, 1962).
[34] W. M. Deen, *Analysis of Transport Phenomena* (Oxford University Press, Oxford, 1998).